Shapley Flow: A Graph-based Approach to Interpreting Model Predictions

Jiaxuan Wang
University of Michigan

Jenna Wiens
University of Michigan

Scott Lundberg
Microsoft Research

Abstract

Many existing approaches for estimating feature importance are problematic because they ignore or hide dependencies among features. A causal graph, which encodes the relationships among input variables, can aid in assigning feature importance. However, current approaches that assign credit to nodes in the causal graph fail to explain the entire graph. In light of these limitations, we propose Shapley Flow, a novel approach to interpreting machine learning models. It considers the entire causal graph, and assigns credit to *edges* instead of treating nodes as the fundamental unit of credit assignment. Shapley Flow is the unique solution to a generalization of the Shapley value axioms to directed acyclic graphs. We demonstrate the benefit of using Shapley Flow to reason about the impact of a model's input on its output. In addition to maintaining insights from existing approaches, Shapley Flow extends the flat, set-based, view prevalent in game theory based explanation methods to a deeper, *graph-based*, view. This graph-based view enables users to understand the flow of importance through a system, and reason about potential interventions.

1 Introduction

Explaining a model's predictions by assigning importance to its inputs (i.e., feature attribution) is critical to many applications in which a user interacts with a model to either make decisions or gain a better understanding of a system (Simonyan et al., 2013; Lundberg and Lee, 2017; Zhou et al., 2016; Shrikumar et al., 2017; Baehrens et al., 2010; Binder et al., 2016; Springenberg et al., 2014; Sundararajan et al., 2017; Fisher et al., 2018; Breiman, 2001). However, correlation among input features presents a challenge when estimating feature importance.

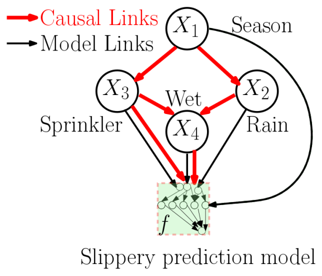

Figure 1: Causal graph for the sprinkler example from (Pearl, 2009, Chapter 1.2). The model, f, can be expanded into its own graph. To simplify the exposition, although f takes 4 variables as input, we arbitrarily assumed that it only depends on X_3 and X_4 directly (*i.e.*, $f(X_1, X_2, X_3, X_4) = g(X_3, X_4)$ for some g).

Consider a motivating example adapted from Pearl (2009), in which we are given a model f that takes as input four features: the season of the year (X_1), whether or not it's raining (X_2), whether the sprinkler is on (X_3), and whether the pavement is wet (X_4) and outputs a prediction $f(\mathbf{x})$, representing the probability that the pavement is slippery (capital X denotes a random variable; lower case $\mathbf{x}$ denotes a particular sample). Assume, the inputs are related through the causal graph in **Figure 1**. When assigning feature importance, existing approaches that ignore this causal structure (Janzing et al., 2020; Sundararajan and Najmi, 2019; Datta et al., 2016) may assign zero importance to the season, since it only indirectly affects the outcome through the other input variables. However, such a conclusion may lead a user astray - since changing X_1 would most definitely affect the outcome.

Recognizing this limitation, researchers have recently proposed approaches that leverage the causal structure among the input variables when assigning credit (Frye et al., 2019). However, such approaches provide an incomplete picture of a system as they assign *all* credit to the source nodes in a graph. Though this solves the earlier problem of ignoring indirect or upstream effects, it does so by ignoring downstream effects. In our example, season would get all the credit despite the importance of the other variables. This again may lead a user astray - since intervening on X_3 or X_4 would affect the outcome, yet they are given no credit.

Given that current approaches end up ignoring either downstream (*i.e.*, direct) or upstream (*i.e.*, indirect) effects, we develop Shapley Flow, a comprehensive approach to interpreting a model (or system) that incorporates the causal relationship among input variables, while accounting for both direct and indirect effects. In contrast to prior work, we accomplish this by reformulating the problem as one related to assigning credit to *edges* in a causal graph, instead of *nodes* (**Figure 2c**). Our key contributions are as follows.

- We propose the first (to the best of our knowledge) generalization of Shapley value feature attribution to graphs, providing a complete system-level view of a model.
- Our approach unifies three previous game theoretic approaches to estimating feature importance.
- Through examples on real data, we demonstrate how our approach facilitates understanding.

In this work, we take an axiomatic approach motivated by cooperative game theory, extending Shapley values to graphs. The resulting algorithm, Shapley Flow, generalizes past work in estimating feature importance (Lundberg and Lee, 2017; Frye et al., 2019; López and Saboya, 2009). The estimates produced by Shapley Flow represent the unique allocation of credit that conforms to several natural axioms. Applied to real-world systems, Shapley Flow can help a user understand both the direct and indirect impact of changing a variable, generating insights beyond current feature attribution methods.

2 Problem Setup & Background

Given a model, or more generally a system, that takes a set of inputs and produces an output, we focus on the problem of quantifying the effect of each input on the output. Here, building off previous work, we formalize the problem setting.

2.1 Problem Setup

Quantifying the effect of each input on a model's output can be formulated as a credit assignment problem.

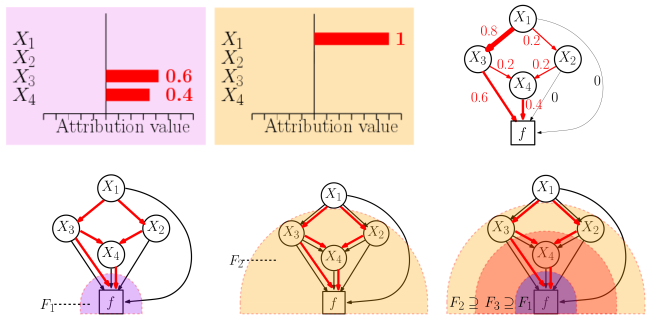

(a) Independent (b) ASV (c) Shapley Flow

Figure 2: Top: Output of attribution methods for the example in **Figure 1**. Bottom: Causal structure (black edges) and explanation boundaries used by each method. As a reference, we copied the true causal links (red) from **Figure 1**. An explanation boundary $\mathcal{B} := (D, F)$ is a cut in the graph that defines a "model" F (nodes in the shaded area in each figure) to explain. Refer to **Section 2.2** for a detailed discussion.

Formally, given a target sample input $\boldsymbol{x}$, a reference sample input $\boldsymbol{x'}$, and a model $f : \mathbb{R}^d \to \mathbb{R}$, we aim to explain the difference in output i.e., $f(\boldsymbol{x}) - f(\boldsymbol{x'})$. We assume $\boldsymbol{x}$ and $\boldsymbol{x'}$ are of the same dimension d, and each entry could be either discrete or continuous.

We also assume access to a causal graph, as formally defined in (Peters et al., 2017, Chapter 6), over the d input variables. Given this graph, we seek an assignment function ϕ that assigns credit $\phi(e) \in \mathbb{R}$ to each edge e in the causal graph such that they collectively explain the difference $f(\boldsymbol{x}) - f(\boldsymbol{x'})$. In contrast with the classical setting (Lundberg and Lee, 2017; Sundararajan et al., 2017; Frye et al., 2020; Aas et al., 2019) in which credit is placed on features (*i.e.*, seeking a node assignment function $\psi(i) \in \mathbb{R}$ for $i \in [1 \cdots d]$), our edge-based approach is more flexible because we can recover node i's importance by defining $\psi(i) = \sum_{e \in \text{i's outgoing edges}} \phi(e)$.

Here, the effect of input on output is measured with respect to a reference or background sample. For example, in a healthcare setting, we may set the features in the background sample to values that are deemed typical for a disease. We assume a single background value for notational convenience, but the formalism easily extends to the common scenario of multiple background values or a distribution of background values, P, by defining the explanation target to be $f(\boldsymbol{x}) - \mathbb{E}_{\boldsymbol{x'} \sim P} f(\boldsymbol{x'})$.

2.2 Feature Attribution with a Causal Graph

Even given a causal graph, feature attribution remains challenging because it is unclear how to rightfully allocate credit for a prediction among the nodes and/or edges of the graph. To address this we generalize game theoretic fairness principles to graphs.

Given a graph, $\mathcal{G}$, that consists of a causal graph over the the model of interest f and its inputs, we define the **boundary of explanation** as a cut $\mathcal{B} := (D, F)$ that partitions the input variables and the output of the model (i.e., the nodes of the graph) into D and F where source nodes (nodes with no incoming edges) are in D and sink nodes (nodes with no outgoing edges) are in F. Note that $\mathcal{G}$ has a single sink, $f(\boldsymbol{x}) \in \mathbb{R}$. A cut set is the set of edges with one endpoint in D and another endpoint in F, denoted as $cut(\mathcal{B})$. It is helpful to think of F as an alternative model definition, where a boundary of explanation (aka. a model boundary) defines what part of the graph we consider to be the "model". If we collapse F into a single node that subsumes f, then $cut(\mathcal{B})$ represents the direct inputs to this new model.

Depending on the causal graph, multiple boundaries of explanation may exist. Recognizing this multiplicity of choices helps shed light on an ongoing debate in the community regarding feature attribution and whether one should perturb features while staying on the data manifold or perturb them independently (Chen et al., 2020; Janzing et al., 2020; Sundararajan and Najmi, 2019). On one side, many argue that perturbing features independently reveals the functional dependence of the model, and is thus *true to the model* (Janzing et al., 2020; Sundararajan and Najmi, 2019; Datta et al., 2016). However, independent perturbation of the data can create unrealistic or invalid sets of model input values. Thus, on the other side, researchers argue that one should perturb features while staying on the data manifold, and so be *true to the data* (Aas et al., 2019; Frye et al., 2019). However, this can result in situations in which features not used by the model are given non-zero attribution. Explanation boundaries help us unify these two viewpoints. As illustrated in **Figure 2a**, when we independently perturb features, we assume the causal graph is flat and the explanation boundary lies between $\boldsymbol{x}$ and f (*i.e.*, D contains all of the input variables). In this example, since features are assumed independent all credit is assigned to the features that directly impact the model output, and indirect effects are ignored (no credit is assigned to X_1 and X_2). In contrast, when we perform on-manifold perturbations with a causal structure, as is the case in Asymmetric Shapley Values (ASV) (Frye et al., 2019), all the credit is assigned to the source node because the source node determines the value of all nodes in the graph (**Figure 2b**). This results in a different boundary of explanation, one between the source nodes and the remainder of the graph. Although giving X_1 credit does not reflect the true functional dependence of f, it does for the model defined by F_2 (**Figure 2c**). Perturbations that were previously faithful to the data are faithful to a "model", just one that corresponds to a different boundary. See **Appendix 6** for how on-manifold perturbation (without a causal graph) can be unified using explanation boundaries.

Beyond the boundary directly adjacent to the model of interest, f, and the boundary directly adjacent to the source nodes, there are other potential boundaries (**Figure 2c**) a user may want to consider. However, simply generating explanations for each possible boundary can quickly overwhelm the user (**Figures 2a 2b 8a**). Our approach sidesteps the issue of selecting a single explanation boundary by considering all explanation boundaries simultaneously. This is made possible by assigning credit to the edges in a causal graph (**Figure 2c**). Edge attribution is strictly more powerful than feature attribution because we can simultaneously capture the direct and indirect impact of edges.

While other approaches to assign credit on a graph exist, (*e.g.*, Conductance from Dhamdhere et al. (2018) and DeepLift from Shrikumar et al. (2016)), they were proposed in the context of understanding internal nodes of a neural network, and depend on implicit linearity and continuity assumptions about the model. We aim to understand the causal structure among the input nodes in a fully model agnostic manner, where discrete variables are allowed, and no differentiability assumption is made. To do this we generalize the widely used Shapley value (Adadi and Berrada, 2018; Mittelstadt et al., 2019; Lundberg et al., 2018; Sundararajan and Najmi, 2019; Frye et al., 2019; Janzing et al., 2020; Chen et al., 2020) to graphs.

3 Proposed Approach: Shapley Flow

Our proposed approach, Shapley Flow, attributes credit to edges of the causal graph. In this section, we present the intuition behind our approach and then formally show that it uniquely satisfies a generalization of the classic Shapley value axioms, while unifying previously proposed approaches.

3.1 Assigning Credit to Edges: Intuition

Given a causal graph defining the relationship among input variables, we re-frame the problem of feature attribution to focus on the edges of a graph rather than nodes. Our approach results in edge credit assignments as shown in **Figure 2c**. As mentioned above, this eliminates the need for multiple explanations (*i.e.*, bar charts) pertaining to each explanation boundary.

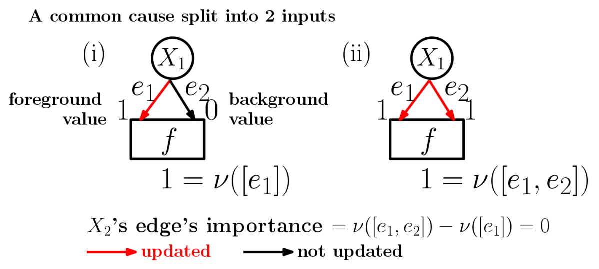

(a) e_2 updates after e_1

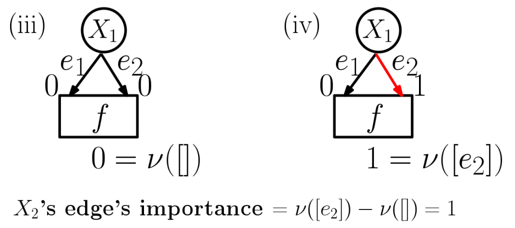

(b) e_2 updates before e_1

Figure 3: Edge importance is measured by the change in output when an edge is added. When a model is non-linear, say $f = OR$, we need to average over all scenarios in which e_2 can be added to gauge its importance. **Section 3.1** has a detailed discussion.

Moreover, it allows a user to better understand the nuances of a system by providing information regarding what would happen if a single causal link breaks.

Shapley Flow is the unique assignment of credit to edges such that classic Shapley value axioms are satisfied for all possible boundaries of explanation. Specifically, we extend the efficiency, dummy, and linearity axioms from (Shapley, 1953) and add a new axiom related to boundary consistency. Efficiency states that the attribution of edges on any boundary must add up to $f(\mathbf{x}) - f(\mathbf{x}')$. Linearity states that explaining a linear combination of models is the same as explaining each model, and linearly combining the resulting attributions. Dummy states that if adding an edge does not change the output in all scenarios, the edge should be assigned 0 credit. Boundary consistency states that edges shared by different boundaries need to have the same attribution when explained using either boundary. These concepts are illustrated in **Figure 4** and formalized in **Section 3.3**.

An edge is important if removing it causes a large change in the model's prediction. However, what does it mean to remove an edge? If we imagine every edge in the graph as a channel that sends its source node's current value to its target node, then removing an edge e simply means messages sent through e fail. In the context of feature attribution, in which we aim to measure the difference between $f(\mathbf{x}) - f(\mathbf{x}')$, this means that e's target node still relies on the source's background value in $\mathbf{x}'$ to update its current value, as opposed to the source node's foreground value in $\mathbf{x}$, as illustrated in **Figure 3a**. However, we cannot simply toggle edges one at a time. Consider a simple OR function $g(X_1, X_2) = X_1 \vee X_2$, with $x_1 = 1$, $x_2 = 1$, $x'_1 = 0$, $x'_2 = 0$. Removing either of the edges alone, would not affect the output and both x_1 and x_2 would be (erroneously) assigned 0 credit.

To account for this, we consider all scenarios (or partial histories) in which the edge we care about can be added (see **Figure 3b**). Here, ν is a function that takes a list of edges and evaluates the network with edges updated in the order specified by the list. For example, $\nu([e_1])$ corresponds to the evaluation of f when only e_1 is updated. Similarly $\nu([e_1, e_2])$ is the evaluation of f when e_1 is updated followed by e_2. The list $[e_1, e_2]$ is also referred to as a (complete) *history* as it specifies how $\mathbf{x}'$ changes to $\mathbf{x}$.

For the same edge, attributions derived from different explanation boundaries should agree, otherwise simply including more details of a model in the causal graph would change upstream credit allocation, even though the model implementation was unchanged. We refer to this property as *boundary consistency*. The Shapley Flow value for an edge is the difference in model output when removing the edge averaged over all histories that are boundary consistent (as defined below).

3.2 Model explanation as value assignments in games

The concept of Shapley value stems from game theory, and has been extensively applied in model interpretability (Štrumbelj and Kononenko, 2014; Datta et al., 2016; Lundberg and Lee, 2017; Frye et al., 2019; Janzing et al., 2020). Before we formally extend it to the context of graphs, we define the credit assignment problem from a game theoretic perspective.

Given the message passing system in **Section 3.1**, we formulate the credit assignment problem as a game specific to an explanation boundary $\mathcal{B} := (D, F)$. The game consists of a set of players $\mathcal{P}_{\mathcal{B}}$, and a payoff function $\nu_{\mathcal{B}}$. We model each edge external to F as a player. A *history* is a list of edges detailing the event from $t = 0$ (values being $\mathbf{x}'$) to $t = T$ (values being $\mathbf{x}$). For example, the history $[i, j, i]$ means that the edge i finishes transmitting a message containing its source node's most recent value to its target node, followed by the edge j, and followed by the edge i again. A *coalition* is a partial history from $t = 0$ to any $t \in [0 \cdots T]$. The *payoff function*, ν, associates each coalition with a real number, and is defined in our case as the evaluation of F following the coalition.

This setup is a generalization of a typical cooperative game in which the ordering of players does not matter

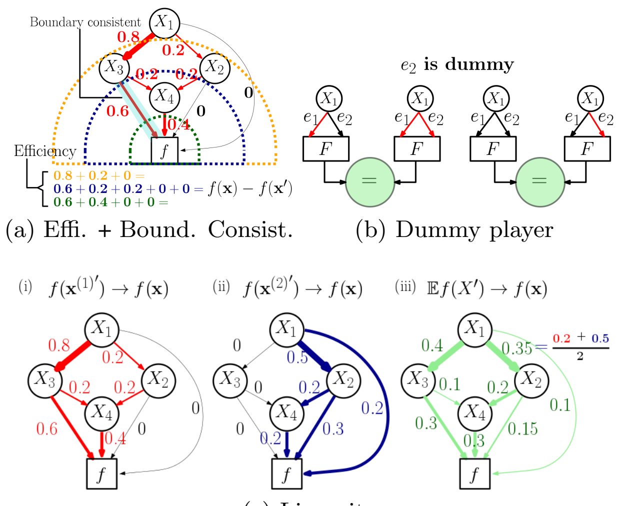

(a) Effi. + Bound. Consist.   (b) Dummy player

(c) Linearity

Figure 4: Illustration for axioms for Shapley Flow. Except for boundary consistency, all axioms stem from Shapley value's axioms (Shapley, 1953). Detailed explanations are included in **Section 3.3**.

(only the set of players matters). However, given our physical system, history is important. In the following sections, we denote '+' as list concatenation, '[]' as an empty coalition, and $\mathcal{H}_{\mathcal{B}}$ as the set of all possible histories. We denote $\tilde{\mathcal{H}}_{\mathcal{B}} \subseteq \mathcal{H}_{\mathcal{B}}$ as the set of boundary consistent histories. The corresponding coalitions for $\mathcal{H}_{\mathcal{B}}$ and $\tilde{\mathcal{H}}_{\mathcal{B}}$ are denoted as $\mathcal{C}_{\mathcal{B}}$ and $\tilde{\mathcal{C}}_{\mathcal{B}}$ respectively. A sample game setup is illustrated in **Figure 3**.

3.3 Axioms

We formally extend the classic Shapley value axioms (efficiency, linearity, and dummy) and include one additional axiom, the boundary consistency axiom, that connects all boundaries together.

- Boundary consistency: for any two boundaries $\mathcal{B}_1 = (D_1, F_1)$ and $\mathcal{B}_2 = (D_2, F_2)$, $\phi_{\nu_{\mathcal{B}_1}}(i) = \phi_{\nu_{\mathcal{B}_2}}(j)$ for $i, j \in cut(\mathcal{B}_1) \cap cut(\mathcal{B}_2)$

  For edges that are shared between boundaries, their attributions must agree. In **Figure 4a**, the edge wrapped by a teal band is shared by both the blue and green boundaries, forcing them to give the same attribution to the edge.

In the general setting, not all credit assignments are boundary consistent; different boundaries could result in different attributions for the same edge. This occurs when histories associated with different boundaries are inconsistent (**Figure 2c**). Moving the boundary from $\mathcal{B}$ to $\mathcal{B}^*$ (where $\mathcal{B}^*$ is the boundary with D containing f's inputs), results in a more detailed set of histories. This expansion has 2 constraints. First, any history in the expanded set must follow the physical system in **Section 3.1**. Second, when a message passes through the boundary, it immediately reaches the end of computation, because F is assumed to be a black-box.

Denoting the history expansion function into $\mathcal{B}^*$ as HE and denoting the set of all boundaries as $\mathcal{M}$, a history h is *boundary consistent* if $\exists h_{\mathcal{B}} \in \mathcal{H}_{\mathcal{B}}$ for all $\mathcal{B} \in \mathcal{M}$ such that

$$\Big(\bigcap_{\mathcal{B}\in\mathcal{M}} HE(h_{\mathcal{B}})\Big) \cap HE(h) \neq \emptyset$$

That is h needs to have a least one fully detailed history in which all boundaries can agree on. $\tilde{\mathcal{H}}$ is all histories in $\mathcal{H}$ that are boundary consistent. We rely on this notion of boundary consistency in generalizing the Shapley axioms to any explanation boundary, $\mathcal{B}$:

- Efficiency: $\sum_{i\in cut(\mathcal{B})} \phi_{\nu_{\mathcal{B}}}(i) = f(\mathbf{x}) - f(\mathbf{x}')$.

  In the general case where $\nu_{\mathcal{B}}$ can depend on the ordering of h, the sum is $\sum_{h\in\tilde{\mathcal{H}}_{\mathcal{B}}} \frac{\nu_{\mathcal{B}}(h)}{|\tilde{\mathcal{H}}_{\mathcal{B}}|} - \nu_{\mathcal{B}}([])$. But when the game is defined by a model function f, $\sum_{h\in\tilde{\mathcal{H}}_{\mathcal{B}}} \nu_{\mathcal{B}}(h)/|\tilde{\mathcal{H}}_{\mathcal{B}}| = f(\boldsymbol{x})$ and $\nu_{\mathcal{B}}([]) = f(\boldsymbol{x}')$. An illustration with 3 boundaries is shown in **Figure 4a**.

- Linearity: $\phi_{\alpha u+\beta v} = \alpha\phi_u + \beta\phi_v$ for any payoff functions u and v and scalars α and β.

  Linearity enables us to compute a linear ensemble of models by independently explaining each model and then linearly weighting the attributions. Similarly, we can explain $f(\mathbf{x}) - \mathbb{E}(f(X'))$ by independently computing attributions for each baseline sample $\mathbf{x}^{(\mathbf{i})\prime}$ and then taking the average of the attributions, without recomputing from scratch whenever the background sample's distribution changes. An illustration with 2 baseline samples is shown in **Figure 4c**.

- Dummy player: $\phi_{\nu_{\mathcal{B}}}(i) = 0$ if $\nu_{\mathcal{B}}(S + [i]) = \nu_{\mathcal{B}}(S)$ for all $S, S + [i] \in \tilde{\mathcal{C}}_{\mathcal{B}}$ for $i \in cut(\mathcal{B})$.

  Dummy player states that if an edge does not change the model's output when added to in all possible coalitions, it should be given 0 attribution. In **Figure 4b**, e_2 is a dummy edge because starting from any coalition, adding e_2 wouldn't change the output.

These last three axioms are extensions of Shapley's axioms. Note that we no longer need the symmetry axiom because it is implied by the updated dummy player with history.

3.4 Shapley Flow is the unique solution

Shapley Flow uniquely satisfies all axioms from the previous section. Here, we describe the algorithm, show its formulae, and state its properties. Please refer to **Appendix 8** and **7** for proofs and code.

Description: Define a configuration of a graph as an arbitrary ordering of outgoing edges of a node when it

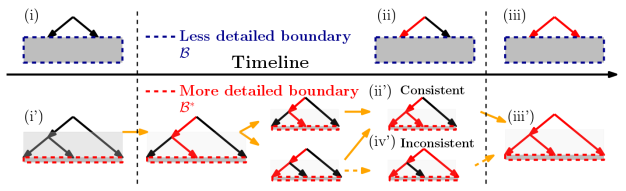

Figure 5: Boundary Consistency. For the blue boundary (upper), we show one potential history h. When we expand h to the red boundary (lower), h corresponds to multiple histories as long as each history contains states that match (i) (ii) and (iii). (i') matches (i), no messages are received in both states. (ii') matches (ii), the full impact of message transmitted through the left edge is received at the end of computation. (iii') matches (iii), all messages are received. In contrast, the history containing (iv') has no state matching (ii), and thus is inconsistent with h.

is traversed by depth first search. For each configuration, we run depth first search starting from the source node, processing edges in the order of the configuration. When processing an edge, we update the value of the edge's target node by making the edge's source node value visible to its function. If the edge's target node is the sink node, the difference in the sink node's output is credited to every edge along the search path from source to sink. The final result averages over attributions for all configurations.

Formulae: Denote the attribution of Shapley Flow to a path as $\tilde{\phi}_\nu$, and the set of all possible orderings of source nodes to a sink path generated by depth first search (DFS) as Π_{dfs}. For each ordering $\pi \in \Pi_{\text{dfs}}$, the inequality of $\pi(j) < \pi(i)$ denotes that path j precedes path i under π. Since ν's input is a list of edges, we define $\tilde{\nu}$ to work on a list of paths. The evaluation of $\tilde{\nu}$ on a list of path is the value of ν evaluated on the corresponding edge traversal ordering. Then

$$\tilde{\phi}_\nu(i) = \sum_{\pi \in \Pi_{\text{dfs}}} \frac{\tilde{\nu}([j : \pi(j) \leq \pi(i)]) - \tilde{\nu}([j : \pi(j) < \pi(i)])}{|\Pi_{\text{dfs}}|} \tag{1}$$

To obtain an edge e's attribution $\phi_\nu(e)$, we sum the path attributions for all paths that contains e.

$$\phi_\nu(e) = \sum_{p \in \text{paths in } \mathcal{G}} \mathbb{1}_{\text{p contains}}(e) \tilde{\phi}_\nu(p) \tag{2}$$

Additional properties: Shapley Flow has the following beneficial properties beyond the axioms.

Generalization of SHAP: if the graph is flat, the edge attribution is equal to feature attribution from SHAP because each input node is paired with a single edge leading to the model.

Generalization of ASV: the attribution to the source nodes is the same as in ASV if all the dependencies among features are modeled by the causal graph.

Generalization of Owen value: if the graph is a tree, the edge attribution for incoming edges to the leaf nodes is the Owen value with a coalition structure defined by the tree.

Implementation invariance: boundary consistency is equivalent to ensuring the attributions are invariant to how f is implemented or modeled.

Conservation of flow: efficiency and boundary consistency imply that the sum of attributions on a node's incoming edges equals the sum of its outgoing edges.

Model agnostic: Shapley Flow can explain arbitrary (non-differentiable) machine learning pipelines.

4 Practical Application

Shapley Flow highlights both the direct and indirect impact of features. In this section, we consider several applications of Shapley Flow. First, in the context of a linear model, we verify that the attributions match our intuition. Second, we show how current feature attribution approaches lead to an incomplete understanding of a system compared to Shapley Flow.

4.1 Experimental Setup

We illustrate the application of Shapley Flow to a synthetic and a benchmark dataset. In addition, we include results for a third dataset in the Appendix. Note that our algorithm assumes a causal graph is provided as input. In recent years there has been significant progress in causal graph estimation (Glymour et al., 2019; Peters et al., 2017). However, since our focus is not on causal inference, we make simplifying assumptions in estimating the causal graphs (see Appendix).

Datasets. *Synthetic*: As a sanity check, we first experiment with synthetic data. We create a random graph dataset with 10 nodes. A node i is randomly connected to node j (with j pointing to i) with 0.5 probability if $i > j$, otherwise 0. The function at each node is linear with weights generated from a standard normal distribution. Sources follow a $N(0, 1)$ distribution. This results in a graph with a single sink node associated with function f (*i.e.*, the 'model' of interest). The remainder of the graph corresponds to the causal structure among the input variables.

National Health and Nutrition Examination Survey: This dataset consists of 9,932 individuals with 18 demographic and laboratory measurements (Cox, 1998). We used the same preprocessing as described by Lundberg et al. (2020). Given these inputs, the model, f, aims to predict survival.

Model training. We train f using an 80/20 random train/test split. For experiments with linear models, f is trained with linear regression. For experiments with non-linear models, f is fitted by 100 XGBoost trees with a max depth of 3 for up to 1000 epochs, using the cox loss.

Causal Graph. We construct a causal graph based on domain knowledge **Figure 9b**. Attributes predetermined at birth (age, race, and sex) are treated as source nodes. Poverty index is placed at the second level because economic status could impact one's health. Other features have directed edges coming from age, race, sex, and poverty index. Note that the relationship among some features is deterministic. For example, pulse pressure is the difference between systolic and diastolic blood pressure. We add the appropriate causal edges to account for such facts. We also account for when features have natural groupings. For example, transferrin saturation (TS), total iron binding capacity (TIBC), and serum iron are all related to blood iron. Serum albumin and serum protein are both blood protein measures. Systolic and diastolic blood pressure can be grouped into blood pressure. Sedimentation rate and white blood cell counts both measure inflammation. We add these higher level grouping concepts as new latent variables in the graph. The resulting causal structure is an oversimplification of the true causal structure; the relationship between source nodes (e.g., race) and biomarkers is far more complex. Nonetheless, it can help in understanding the in/direct effects of input variables on the outcome.

4.2 Baselines

We compare Shapley Flow with other game theoretic feature attribution methods: independent SHAP (Lundberg and Lee, 2017), on-manifold SHAP (Aas et al., 2019), and ASV (Frye et al., 2019), covering both independent and on-manifold feature attribution.

Since Shapley Flow and all baselines are expensive to compute exactly, we use a Monte Carlo approximation of **Equation 1**. In particular, we sample orderings from Π_{dfs} and average across those orderings.We randomly selected a baseline sample from each dataset and share it across methods so that each uses the same baseline. A single baseline allows us to ignore differences in methods due to variations in baseline sampling (A multiple baseline version is easily attainable due to linearity as explained in **Figure 4c**). We sample 100 orderings from each approach to generate the results. Since there's no publicly available implementation for ASV, we show the attribution for source nodes obtained from Shapley Flow (summing attributions of outgoing edges) as they are equivalent given the same causal graph. For convenience of visual inspection, we show top 10 links used by Shapley Flow (credit measured in absolute value) on the nutrition dataset.

Methods	Nutrition (**D**)	Synthetic (**D**)	Nutrition (**I**)	Synthetic (**I**)
Independent	**0.0** (± 0.0)	**0.0** (± 0.0)	0.8 (± 2.7)	1.1 (± 1.4)
On-manifold	1.3 (± 2.5)	0.8 (± 0.7)	0.9 (± 1.6)	1.5 (± 1.5)
ASV	1.5 (± 3.3)	1.2 (± 1.4)	0.6 (± 1.9)	1.1 (± 1.5)
Shapley Flow	**0.0** (± 0.0)	**0.0** (± 0.0)	**0.0** (± 0.0)	**0.0** (± 0.0)

Table 1: Mean absolute error (std) for all methods on direct (**D**) and indirect (**I**) effect for linear models. Shapley Flow makes no mistake across the board.

4.3 Sanity checks with linear models

To build intuition, we first examine linear models (*i.e.*, $f(\mathbf{x}) = \mathbf{w}^\top \mathbf{x} + b$ where $\mathbf{w} \in \mathbb{R}^d$ and $b \in \mathbb{R}$; the causal dependence inside the graph is also linear). When using a linear model the ground truth direct impact of changing feature X_i is $w_i(x_i - x'_i)$ (that is the change in output due to X_i directly), and the ground truth indirect impact is defined as the change in output when an intervention changes x'_i to x_i.

Results for explaining the datasets are included in **Table 1**. We report the mean absolute error from the ground truth attribution for $1,000$ randomly selected examples in both datasets across features. We also report the standard deviation of error in parentheses. Note that only Shapley flow results in no error for both direct and indirect effects.

4.4 Examples with non-linear models

We demonstrate the benefits of Shapley Flow with non-linear models containing both discrete and continuous variables. As a reminder, the baseline methods are not competing with Shapley Flow as the latter can recover all the baselines given the corresponding causal structure (**Figure 2**). Instead, we highlight why a holistic understanding of the system is better.

Independent SHAP ignores the indirect impact of features. Take an example from the nutrition dataset (**Figure 6**). The race feature is given low attribution with independent SHAP, but high importance in ASV. This happens because race, in addition to its direct impact, indirectly affects the output through blood pressure, serum magnesium, and blood protein, as shown by Shapley Flow (**Figure 6a**). In particular, race partially accounts for the impact of serum magnesium because changing race from Black to White on average increases serum magnesium by 0.07 meg/L in the dataset (thus partially explaining the increase in serum magnesium changing from the background sample to the foreground). Independent

SHAP fails to account for the indirect impact of race, leaving the user with a potentially misleading impression that race is irrelevant for the prediction.

On-manifold SHAP provides a misleading interpretation. With the same example (**Figure 6**), we observe that on-manifold SHAP strongly disagrees with independent SHAP, ASV, and Shapley Flow on the importance of age. Not only does it assign more credit to age, it also flips the sign, suggesting that age is protective. However, **Figure 7a** shows that age and earlier mortality are positively correlated; then how could age be protective? **Figure 7b** provides an explanation. Since SHAP considers all partial histories regardless of the causal structure, when we focus on serum magnesium and age, there are two cases: serum magnesium updates before or after age. We focus on the first case because it is where on-manifold SHAP differs from other baselines (all baselines already consider the second case as it satisfies the causal ordering). When serum magnesium updates before age, the expected age given serum magnesium is higher than the foreground age (yellow line above the black marker). Therefore when age updates to its foreground value, we observe a decrease in age, leading to a decrease in the output (so age appears to be protective). Serum magnesium is just one variable from which age steals credit. Similar logic applies to TIBC, red blood cells, serum iron, serum protein, serum cholesterol, and diastolic BP. From both an in/direct impact perspective, on-manifold perturbation can be misleading since it is based not on causal but on observational relationships.

ASV ignores the direct impact of features. As shown in **Figure 6**, serum magnesium appears to be more important in independent SHAP compared to ASV. From Shapley Flow (**Figure 6a**), this difference is explained by race as its edge to serum magnesium has a negative impact. However, looking at ASV alone, one fails to understand that intervening on serum magnesium could have a larger impact on the output.

Shapley Flow shows both direct and indirect impacts of features. Focusing on the attribution given by Shapley Flow (**Figure 6a**). We not only observe similar direct impacts in variables compared to independent SHAP, but also can trace those impacts to their source nodes, similar to ASV. Furthermore, Shapley Flow provides more detail compared to other approaches. For example, using Shapley Flow we gain a better understanding of the ways in which race impacts survival. The same goes for all other features. This is useful because causal links can change (or break) over time. Our method provides a way to reason through the impact of such a change.

We provide more examples and an additional dataset highlighting the utility of Shapley Flow in the Appendix.

Top features	Age	Serum Magnesium	Race
Background sample	35.0	1.37	Black
Foreground sample	42.0	1.63	white

Attributions	Independent	On-manifold	ASV
Age	0.23	-0.38	0.3
Serum Magnesium	-0.21	-0.02	-0.15
Race	-0.06	0.04	-0.24
Pulse pressure	0.0	-0.08	0.0
Diastolic BP	0.0	0.08	0.0
Serum Cholesterol	0.0	0.07	0.0
Serum Protein	0.01	0.06	0.0
Serum Iron	0.0	0.05	0.0
Poverty index	-0.02	0.01	-0.01
Systolic BP	-0.03	-0.01	0.0

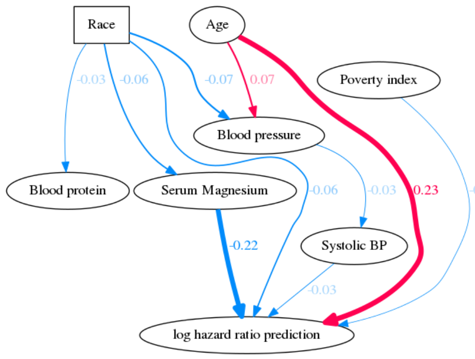

(a) Shapley Flow

Figure 6: Comparison among baselines on a sample (top table) from the nutrition dataset, showing top 10 features/edges.

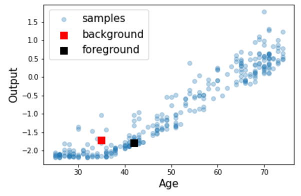

(a) Age vs. output

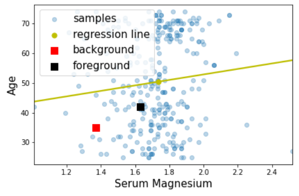

(b) Age vs. magnesium

Figure 7: Age appears to be protective in on-manifold SHAP because it steals credit from other variables.

5 Conclusion

We extend the classic Shapley value axioms to causal graphs, resulting in a unique edge attribution method: Shapley Flow. It unifies three previous Shapley value based feature attribution methods, and enables the joint understanding of both the direct and indirect impact of features. This more comprehensive understanding is useful when interpreting any machine learning model, both ‘black box’ methods, and ‘interpretable’ methods.

References

Aas, K., Jullum, M., and Løland, A. (2019). Explaining individual predictions when features are dependent: More accurate approximations to shapley values. *arXiv preprint arXiv:1903.10464*.

Adadi, A. and Berrada, M. (2018). Peeking inside the black-box: A survey on explainable artificial intelligence (xai). *IEEE Access*, 6:52138–52160.

Baehrens, D., Schroeter, T., Harmeling, S., Kawanabe, M., Hansen, K., and Müller, K.-R. (2010). How to explain individual classification decisions. *The Journal of Machine Learning Research*, 11:1803–1831.

Binder, A., Montavon, G., Lapuschkin, S., Müller, K.-R., and Samek, W. (2016). Layer-wise relevance propagation for neural networks with local renormalization layers. In *International Conference on Artificial Neural Networks*, pages 63–71. Springer.

Breiman, L. (2001). Random forests. *Machine learning*, 45(1):5–32.

Chen, H., Janizek, J. D., Lundberg, S., and Lee, S.-I. (2020). True to the model or true to the data? *arXiv preprint arXiv:2006.16234*.

Cox, C. S. (1998). *Plan and operation of the NHANES I Epidemiologic Followup Study, 1992*. Number 35. National Ctr for Health Statistics.

Datta, A., Sen, S., and Zick, Y. (2016). Algorithmic transparency via quantitative input influence: Theory and experiments with learning systems. In *2016 IEEE symposium on security and privacy (SP)*, pages 598–617. IEEE.

Dhamdhere, K., Sundararajan, M., and Yan, Q. (2018). How important is a neuron? *arXiv preprint arXiv:1805.12233*.

Fisher, A., Rudin, C., and Dominici, F. (2018). All models are wrong but many are useful: Variable importance for black-box, proprietary, or misspecified prediction models, using model class reliance. *arXiv preprint arXiv:1801.01489*, pages 237–246.

Frye, C., de Mijolla, D., Cowton, L., Stanley, M., and Feige, I. (2020). Shapley-based explainability on the data manifold. *arXiv preprint arXiv:2006.01272*.

Frye, C., Feige, I., and Rowat, C. (2019). Asymmetric shapley values: incorporating causal knowledge into model-agnostic explainability. *arXiv preprint arXiv:1910.06358*.

Glymour, C., Zhang, K., and Spirtes, P. (2019). Review of causal discovery methods based on graphical models. *Frontiers in genetics*, 10:524.

Janzing, D., Minorics, L., and Blöbaum, P. (2020). Feature relevance quantification in explainable ai: A causal problem. In *International Conference on Artificial Intelligence and Statistics*, pages 2907–2916. PMLR.

López, S. and Saboya, M. (2009). On the relationship between shapley and owen values. *Central European Journal of Operations Research*, 17(4):415.

Lundberg, S. M., Erion, G., Chen, H., DeGrave, A., Prutkin, J. M., Nair, B., Katz, R., Himmelfarb, J., Bansal, N., and Lee, S.-I. (2020). From local explanations to global understanding with explainable ai for trees. *Nature machine intelligence*, 2(1):2522–5839.

Lundberg, S. M., Erion, G. G., and Lee, S.-I. (2018). Consistent individualized feature attribution for tree ensembles. *arXiv preprint arXiv:1802.03888*.

Lundberg, S. M. and Lee, S.-I. (2017). A unified approach to interpreting model predictions. In *Advances in neural information processing systems*, pages 4765–4774.

Mittelstadt, B., Russell, C., and Wachter, S. (2019). Explaining explanations in ai. In *Proceedings of the conference on fairness, accountability, and transparency*, pages 279–288.

Pearl, J. (2009). *Causality*. Cambridge university press.

Peters, J., Janzing, D., and Schölkopf, B. (2017). *Elements of causal inference*. The MIT Press.

Shapley, L. S. (1953). A value for n-person games. *Contributions to the Theory of Games*, 2(28):307–317.

Shrikumar, A., Greenside, P., and Kundaje, A. (2017). Learning important features through propagating activation differences. *arXiv preprint arXiv:1704.02685*.

Shrikumar, A., Greenside, P., Shcherbina, A., and Kundaje, A. (2016). Not just a black box: Learning important features through propagating activation differences. *arXiv preprint arXiv:1605.01713*.

Simonyan, K., Vedaldi, A., and Zisserman, A. (2013). Deep inside convolutional networks: Visualising image classification models and saliency maps. *arXiv preprint arXiv:1312.6034*.

Springenberg, J. T., Dosovitskiy, A., Brox, T., and Riedmiller, M. (2014). Striving for simplicity: The all convolutional net. *arXiv preprint arXiv:1412.6806*.

Štrumbelj, E. and Kononenko, I. (2014). Explaining prediction models and individual predictions with feature contributions. *Knowledge and information systems*, 41(3):647–665.

Sundararajan, M. and Najmi, A. (2019). The many shapley values for model explanation. *arXiv preprint arXiv:1908.08474*.

Sundararajan, M., Taly, A., and Yan, Q. (2017). Axiomatic attribution for deep networks. *International Conference on Machine Learning*.

Zhou, B., Khosla, A., Lapedriza, A., Oliva, A., and Torralba, A. (2016). Learning deep features for discriminative localization. In *Proceedings of the IEEE conference on computer vision and pattern recognition*, pages 2921–2929.

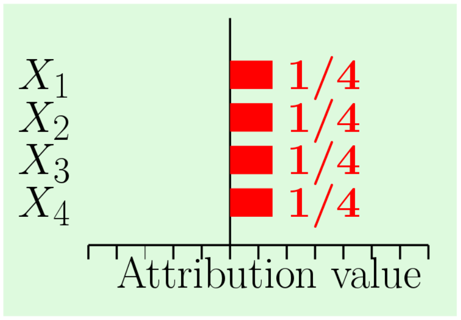

(a) On-manifold attribution

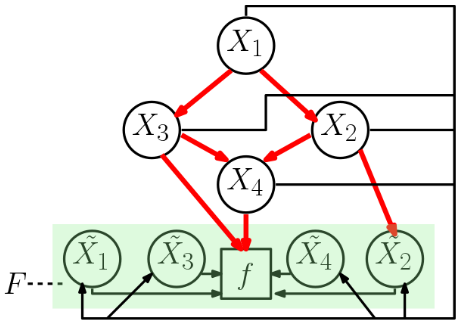

(b) On-manifold boundary

Figure 8: On manifold perturbation methods can be computed using Shapley Flow with a specific explanation boundary.

6 Explanation boundary for on-manifold methods without a causal graph

On-manifold perturbation using conditional expectations can be unified with Shapley Flow using explanation boundaries (**Figure 8a**). Here we introduce $\tilde{X_i}$ as an auxiliary variable that represent the imputed version of X_i. Perturbing any feature X_i affects all input to the model ($\tilde{X_1}$, $\tilde{X_2}$, $\tilde{X_3}$, $\tilde{X_4}$) so that they respect the correlation in the data after the perturbation. When X_i has not been perturbed, $\tilde{X_j}$ treats it as missing for $i, j \in [1, 2, 3, 4]$ and would sample $\tilde{X_j}$ from the conditional distribution of X_j given non-missing predecessors. The red edges contain causal links from **Figure 1**, whereas the black edges are the causal structure used by the on-manifold perturbation method. The credit is equally split among the features because they are all correlated. Again, although giving X_1 and X_2 credit is not true to f, it is true to the model defined by F.

7 The Shapley Flow algorithm

A pseudo code implementation highlighting the main ideas for Shapley Flow is included in **Algorithm 1**. For approximations, instead of trying all edge orderings in line 15 of **Algorithm 1**, one can try random orderings and average over the number of orderings tried. We will release the code.

8 Shapley Flow's uniqueness proof

Without loss of generality, we can assume $\mathcal{G}$ has a single source node s. We can do this because every node in a causal graph is associated with an independent noise node (Peters et al., 2017, Chapter 6). For deterministic relationships, the function for a node doesn't depend on its noise. Treating those noise node as a single node, s, wouldn't have changed any boundaries that already exist in the original graph. Therefore we can assume there is a single source node s.

8.1 At most one solution satisfies the axioms

Assuming that a solution exists, we show that it must be unique.

Proof. We adapt the argument from the Shapley value uniqueness proof [1], by defining basis payoff functions as carrier games. Choose any boundary $\mathcal{B}$, we show here that any game defined on the boundary is unique. We also drop the subscript $\mathcal{B}$ in the proof as there is no ambiguity. Note that since every edge will appear in some boundary, if all boundary edges are uniquely attributed to, all edges have unique attributions. A carrier game associated with coalition (ordered list) O is a game with payoff function v^O such that $v^O(S) = 1(0)$ if coalition S starts with O (otherwise 0). By dummy player, we know that only the last edge e in O gets credit and all other edges in the cut set are dummy because a coalition is constructed in order (only adding e changes the payoff from 0 to 1). Note that e must be an edge in the boundary to form a valid game because boundary edges are

[1] `https://ocw.mit.edu/courses/economics/14-126-game-theory-spring-2016/lecture-notes/MIT14_126S16_cooperative.pdf`

Algorithm 1 Shapley Flow pseudo code

Input: A computational graph $\mathcal{G}$ (each node i has a function f_i), foreground sample $\mathbf{x}$, background sample $\mathbf{x}'$
Output: Edge attribution $\phi : E \to \mathbb{R}$
Initialization:
$\mathcal{G}$: add an new source node pointing to original source nodes.

```
 1: function ShapleyFlow($\mathcal{G}$, $\mathbf{x}'$, $\mathbf{x}$)
 2:     Initialize($\mathcal{G}$, $\mathbf{x}'$, $\mathbf{x}$)                    ▷ Set up game $v$ for any boundary in $\mathcal{G}$
 3:     $s \leftarrow$ source($\mathcal{G}$)                                  ▷ Obtain the source node
 4:     return DFS($s$, {}, [])
 5: end function

 6: function DFS($s$, $D$, $S$)
 7:     ▷ $s$ is a node, $D$ is the data side of the current boundary, $S$ is coalition
 8:     ▷ Using Python list slice notation
 9:     Initialize $\phi$ to output 0 for all edges
10:     if IsSinkNode(s) then
11:         ▷ Here we overload $D$ to refer to its boundary
12:         $\phi(S[-1]) \leftarrow v_D(S) - v_D(S[:-1])$      ▷ Difference in output is attributed to the edge
13:         return $\phi$
14:     end if

15:     for $p \leftarrow$ AllOrderings(Children($s$)) do     ▷ Try all orderings/permutations of the node's children
16:         for $c \leftarrow p$ do                            ▷ Follow the permutation to get the node one by one
17:             edgeCredit $\leftarrow$ DFS($c$, $D \cup \{s\}$, $S + [(s, c)]$)                  ▷ Recurse downward

18:             $\phi \leftarrow \phi + \frac{\text{edgeCredit}}{\text{NumChildren}(s)!}$             ▷ Average attribution over number of runs
19:             $\phi(S[-1]) \leftarrow \phi(S[-1]) + \frac{\text{edgeCredit}(s,c)}{\text{NumChildren}(s)!}$      ▷ Propagate upward
20:         end for
21:     end for
22:     return $\phi$
23: end function
```

the only edges that are connected to the model defined by the boundary. Therefore we give 0 credit to edges in the cut set other than e (because they are *dummy players*). By the *efficiency axiom*, we give $1/|\tilde{\mathcal{H}}|$ credit to e where $\tilde{\mathcal{H}}$ is the set of all possible boundary consistent histories as defined in **Section 3.3**. This uniquely attributed the boundary edges for this game.

We show that the set of carrier games associated with every coalition that ends in a boundary edge (denoted as $\hat{C}$) form basis functions for all payoff functions associated with the system. Recall from **Section 3.2** that $\tilde{C}$ is the set of *boundary consistent coalitions*. We show here that payoff value on coalitions from $\tilde{C}$ is redundant given $\hat{C}$. Note that $\tilde{C} \backslash \hat{C}$ represents all the coalitions that do not end in a boundary edge. For $c \in \tilde{C} \backslash \hat{C}$, $v^O(c) = v^O(c[:-1])$ (using Python's slice notation on list) because only boundary edges are connected to the model defined by the boundary. Therefore it suffices to show that v^O is linearly independent for $O \in \hat{C}$. For a contradiction, assume for all $c \in \hat{C}$, $\sum_{O \subseteq \hat{C}} \alpha^O v^O(c) = 0$, with some non zero $\alpha^O \in \mathbb{R}$ (definition of linear dependence). Let S be a coalition with minimal length such that $\alpha^S \neq 0$. We have $\sum_{O \subseteq \hat{C}} \alpha^O v^O(S) = \alpha^S$, a contradiction.

Therefore for any v we have unique α's such that $v = \sum_{O \subseteq \hat{C}} \alpha^O v^O$. Using the *linearity axiom*, we have

$$\phi_v = \phi_{\sum_{O \subseteq \hat{C}} \alpha^O v^O} = \sum_{O \subseteq \hat{C}} \alpha^O \phi_{v^O}$$

The uniqueness of α and ϕ_{v^O} makes the attribution unique if a solution exists. Axioms used in the proof are italicized.

□

8.2 Shapley Flow satisfy the axioms

Proof. We first demonstrate how to generate all boundaries. Then we show that Shapley Flow gives boundary consistent attributions. Following that, we look at the set of histories that can be generated by DFS in boundary $\mathcal{B}$, denoted as $\Pi^{\text{dfs}}_{\mathcal{B}}$. We show that $\Pi^{\text{dfs}}_{\mathcal{B}} = \tilde{\mathcal{H}}_{\mathcal{B}}$. Using this fact, we check the axioms one by one.

- Every boundary can be "grown" one node at a time from $D = \{s\}$ where s is the source node: Since the computational graph $\mathcal{G}$ is a directed acyclic graph (DAG), we can obtain a topological ordering of the nodes in $\mathcal{G}$. Starting by including the first node in the ordering (the source node s), which defines a boundary as $(D = \{s\}, F = \text{Nodes}(\mathcal{G}) \backslash D)$, we grow the boundary by adding nodes to D (removing nodes from F) one by one following the topological ordering. This ordering ensures the corresponding explanation boundary is valid because the cut set only flows from D to F (if that's not true, then one of the dependency nodes is not in D, which violates topological ordering).

  Now we show every boundary can be "grown" in this fashion. In other words, starting from an arbitrary boundary $\mathcal{B}_1 = (D_1, F_1)$, we can "shrink" one node at a time to $D = \{s\}$ by reversing the growing procedure. First note that, D_1 must have a node with outgoing edges only pointing to nodes in F_1 (if that's not the case, we have a cycle in this graph because we can always choose to go through edges internal to D_1 and loop indefinitely). Therefore we can just remove that node to arrive at a new boundary (now its incoming edges are in the cut set). By the same argument, we can keep removing nodes until $D = \{s\}$, completing the proof.

- Shapley Flow gives boundary consistent attributions: We show that every boundary grown has edge attribution consistent with the previous boundary. Therefore all boundaries have consistent edge attribution because the boundary formed by any two boundary's common set of nodes can be grown into those two boundaries using the property above. Let's focus on the newly added node c from one boundary to the next. Note that a property of depth first search is that every time c's value is updated, its outgoing edges are activated in an atomic way (no other activation of edges occur between the activation of c's outgoing edges). Therefore, the change in output due to the activation of new edges occur together in the view of edges upstream of c, thus not changing their attributions. Also, since c's outgoing edges must point to the model defined by the current boundary (otherwise it cannot be a valid topological ordering), they don't have down stream edges, concluding the proof.

- $\Pi_{\mathcal{B}}^{\text{dfs}} = \tilde{\mathcal{H}}_{\mathcal{B}}$: Since attribution is boundary consistent, we can treat the model as a blackbox and only look at the DFS ordering on the data side. Observe that the edge traversal ordering in DFS is a valid history because a) every edge traversal can be understood as a message received through edge , b) when every message is received, the node's value is updated, and c) the new node's value is sent out through every outgoing edge by the recursive call in DFS. Therefore the two side of the equation are at least holding the same type of object.

  We first show that $\Pi_{\mathcal{B}}^{\text{dfs}} \subseteq \tilde{\mathcal{H}}_{\mathcal{B}}$. Take $h \in \Pi_{\mathcal{B}}^{\text{dfs}}$, we need to find a history h^* in $\mathcal{B}^*$ such that a) h can be expanded into h^* and b) for any boundary, there is a history in that boundary that can be expanded into h^*. Let h^* be any history expanded using DFS that is aligned with h. To show that every boundary can expand into h^*, we just need to show that the boundaries generated through growing process introduced in the first bullet point can be expanded into h^*. The base case is $D = \{s\}$. There must have an ordering to expand into h^* because h^* is generated by DFS, and that DFS ensures that every edge's impact on the boundary is propagated to the end of computation before another edge in D is traversed. Similarly, for the inductive step, when a new node c is added, we just follow the expansion of its previous boundary to reach h^*.

  Next we show that $\tilde{\mathcal{H}}_{\mathcal{B}} \subseteq \Pi_{\mathcal{B}}^{\text{dfs}}$. First observe that for history h_1 in $\mathcal{B}_1 = (D_1, F_1)$ and history h_2 in $\mathcal{B}_2 = (D_2, F_2)$ with $F_2 \subseteq F_1$, if h_1 cannot be expanded into h_2, then $HE(h_1) \cap HE(h_2) = \emptyset$ because they already have mismatches for histories that doesn't involve passing through $\mathcal{B}_1$. Assume we do have $h \in \tilde{\mathcal{H}}_{\mathcal{B}}$ but $h \notin \Pi_{\mathcal{B}}^{\text{dfs}}$. To derive a contradiction, we shrink the boundary one node at a time from $\mathcal{B}$, again using the procedure described in the first bullet point. We denote the resulting boundary formed by removing n nodes as $\mathcal{B}_{-n}$. Since h is assumed to be boundary consistent, there exist $h_{\mathcal{B}_{-1}} \in \tilde{\mathcal{H}}_{\mathcal{B}_{-1}}$ such that $h_{\mathcal{B}_{-1}}$ must be able to expand into h. Say the two boundaries differ in node c. Note that any update to c crosses $\mathcal{B}_{-1}$, therefore its impact must be reached by F before another event occurs in D_{-1}. Since all of c's outgoing edges crosses $\mathcal{B}$, any ordering of messages sent through those edges is a DFS ordering from c. This means that if $h_{\mathcal{B}_{-1}}$ can be reached by DFS, so can $h_{\mathcal{B}}$, violating the assumption. Therefore, $h_{\mathcal{B}_{-1}} \notin \Pi_{\mathcal{B}_{-1}}^{\text{dfs}}$ and $h_{\mathcal{B}_{-1}} \notin \tilde{\mathcal{H}}_{\mathcal{B}_{-1}}$ (the latter because $h_{\mathcal{B}_{-1}}$ can expand into a history that is consistent with all boundaries by first expanding into h). We run the same argument until $D = \{s\}$. This gives a contradiction because in this boundary, all histories can be produced by DFS.

- Efficiency: Since we are attributing credit by the change in the target node's value following a history h given by DFS, the target for this particular DFS run is thus $v_{\mathcal{B}}(h) - v_{\mathcal{B}}([])$. Average over all DFS runs and noting that $\tilde{\mathcal{H}}_{\mathcal{B}} = \Pi_{\mathcal{B}}^{\text{dfs}}$ gives the target $\sum_{h \in \tilde{\mathcal{H}}_{\mathcal{B}}} v_{\mathcal{B}}(h)/|\tilde{\mathcal{H}}_{\mathcal{B}}| - v_{\mathcal{B}}([])$. Noting that each update in the target node's value must flow through one of the boundary edges. Therefore the sum of boundary edges' attribution equals to the target.

- Linearity: For two games of the same boundary v and u, following any history, the sum of output differences between the two games is the output difference of the sum of the two games, therefore ϕ_{v+u} would not differ from $\phi_v + \phi_u$. It's easy to see that extending addition to any linear combination wouldn't matter.

- Dummy player: Since Shapley Flow is boundary consistent, we can just run DFS up to the boundary (treat F as a blackbox). Since every step in DFS remains in the coalition $\tilde{\mathcal{C}}_{\mathcal{B}}$ because $\Pi_{\mathcal{B}}^{\text{dfs}} \subseteq \tilde{\mathcal{H}}_{\mathcal{B}}$, if an edge is dummy, every time it is traversed through DFS, the output won't change by definition, thus giving it 0 credit.

□

Therefore Shapley Flow uniquely satisfies the axioms. We note that efficiency requirement simplifies to $f(\boldsymbol{x}) - f(\boldsymbol{x'})$ when applying it to an actual model because all histories from DFS would lead the target node to its target value. We can prove a stronger claim that actually all nodes would reach its target value when DFS finishes. To see that, we do an induction on a topological ordering of the nodes. The source nodes reaches its final value by definition. Assume this holds for the k^{th} node. For the $k + 1^{\text{th}}$ node, its parents achieves target value by induction. Therefore DFS would make the parents' final values visible to this node, thus updating it to the target value.

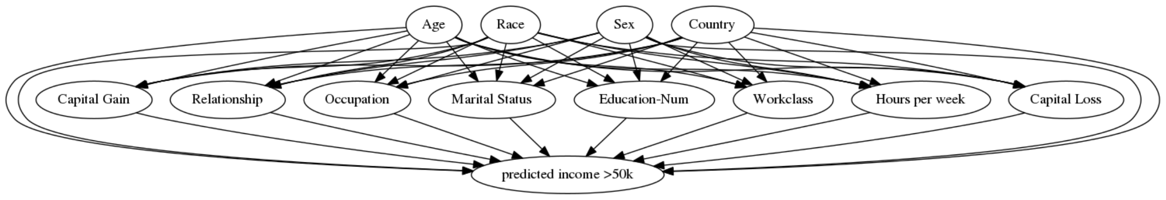

(a) Causal graph for the Census Income dataset

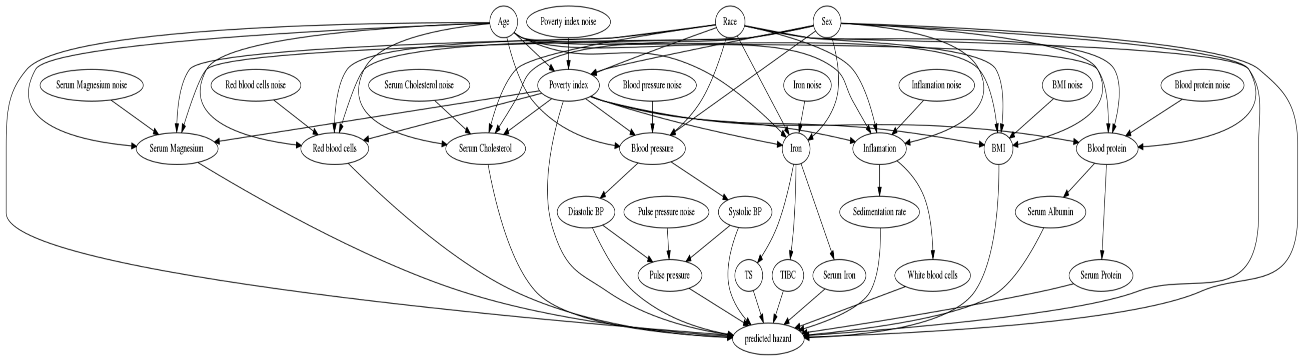

(b) Causal graph for the nutrition dataset

Figure 9: The causal graphs we used for the two real datasets.

9 Causal graphs

While the nutrition dataset is introduced in the main text, we describe an additional dataset to further demonstrate the usefulness of Shapley Flow. Moreover, we describe in detail how the causal relationship is estimated. The resulting causal graphs for the nutrition dataset and the income dataset are visualized in **Figure 9**.

9.1 The Census Income dataset

The Census Income dataset consists of $32,561$ samples with 12 features. The task is to predict whether one's annual income exceeds $50k$. We assume a causal graph, similar to that used by Frye et al. (2019) (**Figure 9a**). Attributes determined at birth e.g., sex, native country, and race act as source nodes. The remaining features (marital status, education, relationship, occupation, capital gain, work hours per week, capital loss, work class) have fully connected edges pointing from their causal ancestors. All features have a directed edge pointing to the model.

9.2 Causal Effect Estimation

Given the causal structure described above, we estimate the relationship among variables using XGBoost. More specifically, using an 80/20 train test split, we use XGBoost to learn the function for each node. If the node value is categorical, we train minimize cross entropy loss. Otherwise, they we minimize mean squared error. Models are fitted by 100 XGBoost trees with a max depth of 3 for up to 1000 epochs. Since features are rarely perfectly determined by their dependency node, we add independent noise nodes to account for this effect. That is, each non-sink node is pointed to by a unique noise node that account for the residue effect of the prediction.

Depending on whether the variable is discrete or continuous, we handle the noise differently. For continuous variables, the noise node's value is the residue between the prediction and the actual value. For discrete variables, we assume the actual value is sampled from the categorical distribution specified by the prediction. Therefore the noise node's value is any possible random number that could result in the actual value.

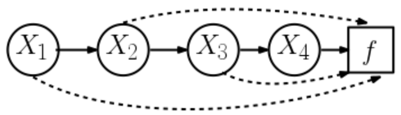

(a) chain dataset

	Independent	On-manifold	ASV
X4	-1.82	-0.45	0.0
X1	0.0	-0.45	-1.82
X3	0.0	-0.45	0.0
X2	0.0	-0.45	0.0

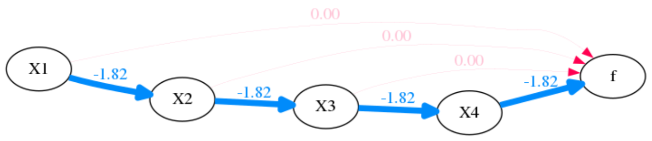

(b) Shapley Flow

Figure 10: **(a)** The chain dataset contains exact copies of nodes. The dashed edges denotes dummy dependencies. **(b)** While Shapley Flow shows the entire path of influence, other baselines fails to capture either direct and indirect effects.

Methods	Income	Nutrition	Synthetic
Independent	**0.0** (± 0.0)	**0.0** (± 0.0)	**0.0** (± 0.0)
On-manifold	0.4 (± 0.3)	1.3 (± 2.5)	0.8 (± 0.7)
ASV	0.4 (± 0.6)	1.5 (± 3.3)	1.2 (± 1.4)
Shapley Flow	**0.0** (± 0.0)	**0.0** (± 0.0)	**0.0** (± 0.0)

Table 2: Shapley Flow and independent SHAP have lower mean absolute error (std) for direct effect of features on linear models.

10 Additional Results

In this section, we first present additional sanity checks with synthetic data. Then we show additional examples from both the nutrition and income datasets to demonstrate how a complete view of boundaries should be preferable over single boundary approaches.

10.1 Additional Sanity Checks

We include further sanity check experiments in this section. The first sanity check consists of a chain with 4 variables. Each node along the chain is an identical copy of its predecessor and the function to explain only depends on X_4 (**Figure 10**). The dataset is created by sampling $X_1 \sim \mathcal{N}(0, 1)$, that is a standard normal distribution, with 1000 samples. We use the first sample as baseline, and explain the second sample (one can choose arbitrary samples to obtain the same insights). As shown in **Figure 10**, independent SHAP fails to show the indirect impact of X_1, X_2, and X_3, ASV fails to show the direct impact of X_4, on manifold SHAP fails to fully capture both the direct and indirect importance of any edge.

The second sanity check consists of linear models as described in 4.3. We include the full result with the income

Methods	Income	Nutrition	Synthetic
Independent	0.1 (± 0.2)	0.8 (± 2.7)	1.1 (± 1.4)
On-manifold	0.4 (± 0.3)	0.9 (± 1.6)	1.5 (± 1.5)
ASV	0.1 (± 0.1)	0.6 (± 1.9)	1.1 (± 1.5)
Flow	**0.0** (± 0.0)	**0.0** (± 0.0)	**0.0** (± 0.0)

Table 3: Shapley Flow and ASV have lower mean absolute error (std) for indirect effect on linear models.

dataset added in **Table 2** and **Table 3** for direct and indirect effects respectively. The trend for the income dataset algins with the nutrition and synthetic dataset: only Shapley Flow makes no mistake for estimating both direct and indirect impact. Independent Shap only does well for direct effect. ASV only does well for indirect effects (it only reaches zero error when evaluated on source nodes).

10.2 Additional examples

Figure 11 gives an example of applying Shapley Flow and baselines on the income dataset. Note that the attribution to capital gain drops from independent SHAP to on-manifold SHAP and ASV. From Shapley Flow, we know the decreased attribution is due to age and race. More examples are shown in **Figure 12 13**.

10.3 A global understanding with Shapley Flow

In addition to explaining a particular example, one can explain an entire dataset with Shapley Flow. Specifically, for multi-class classification problems, we take the average of attributions for the probability predicted for the actual class, in accordance with (Frye et al., 2019). A demonstration on the income dataset using 1000 randomly selected examples is included in **Figure 14**. As before, we use a single shared background sample for explanation. Here, we observe that although the relative importance across independent SHAP, on-manifold SHAP, and ASV are similar, age and sex have opposite direct versus indirect impact as shown by Shapley Flow.

	Background sample	Foreground sample
Age	39	35
Workclass	State-gov	Federal-gov
Education-Num	13	5
Marital Status	Never-married	Married-civ-spouse
Occupation	Adm-clerical	Farming-fishing
Relationship	Not-in-family	Husband
Race	White	Black
Sex	Male	Male
Capital Gain	2174	0
Capital Loss	0	0
Hours per week	40	40
Country	United-States	United-States

	Independent	On-manifold	ASV
Education-Num	-0.12	-0.11	-0.09
Relationship	0.05	0.06	0.04
Capital Gain	0.09	0.01	0.03
Occupation	-0.03	-0.07	-0.02
Marital Status	0.04	0.05	0.03
Workclass	0.02	0.03	0.02
Race	-0.01	-0.03	0.01
Age	-0.01	-0.01	0.02
Capital Loss	0.0	0.03	0.0
Country	0.0	0.03	0.0
Sex	0.0	0.03	0.0
Hours per week	0.0	0.0	0.0

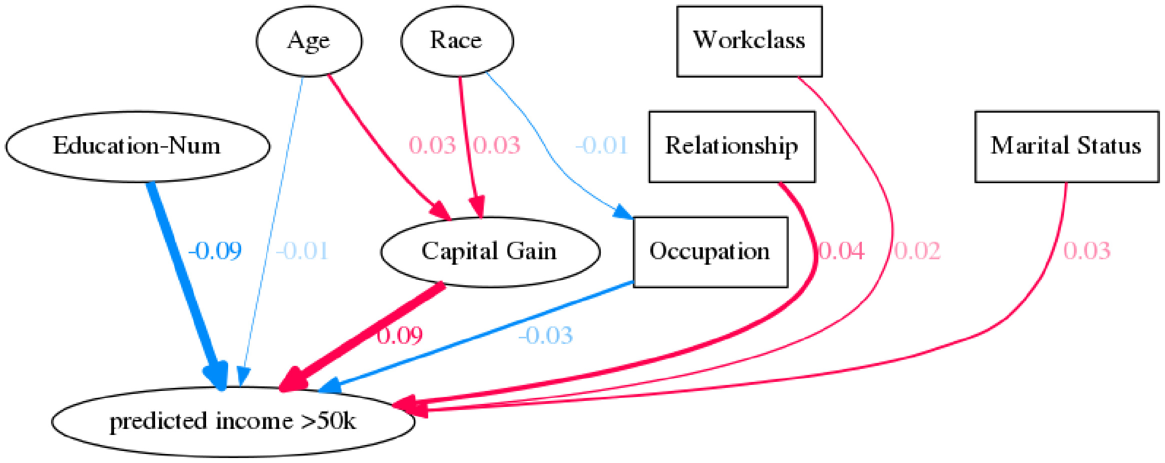

(a) Shapley Flow

Figure 11: Comparison between independent SHAP, on-manifold SHAP, ASV, and Shapley Flow on a sample from the income dataset. Shapley flow shows the top 10 links. The direct impact of capital gain is not represented by independent and on-manifold SHAP.

	Background sample	foreground sample
Age	39	30
Workclass	State-gov	State-gov
Education-Num	13	13
Marital Status	Never-married	Married-civ-spouse
Occupation	Adm-clerical	Prof-specialty
Relationship	Not-in-family	Husband
Race	White	Asian-Pac-Islander
Sex	Male	Male
Capital Gain	2174	0
Capital Loss	0	0
Hours per week	40	40
Country	United-States	India

	Independent	On-manifold	ASV
Relationship	0.17	0.04	0.13
Capital Gain	0.22	0.01	0.07
Occupation	0.1	0.06	0.07
Marital Status	0.08	0.06	0.07
Country	-0.04	0.07	0.07
Age	-0.0	-0.02	0.13
Education-Num	0.0	0.12	0.0
Race	0.02	0.07	0.0
Workclass	0.0	0.06	0.0
Hours per week	0.0	0.03	0.0
Sex	0.0	0.03	0.0
Capital Loss	0.0	0.01	0.0

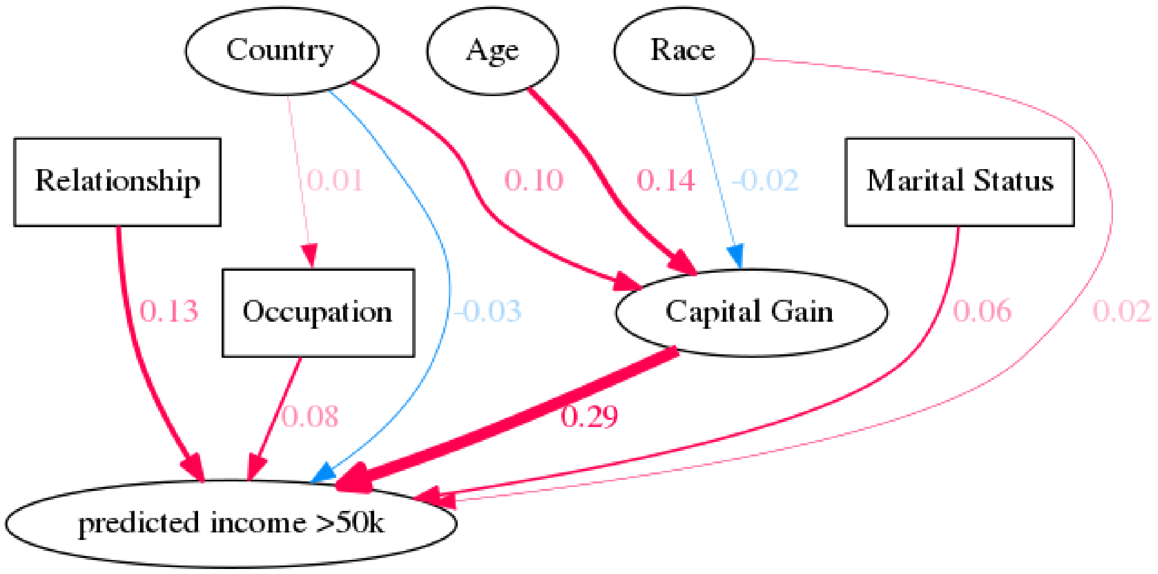

(a) Shapley Flow

Figure 12: Comparison between independent SHAP, on-manifold SHAP, ASV, and Shapley Flow on a sample from the income dataset. Shapley flow shows the top 10 links. The indirect impact of age is only highlighted by Shapley Flow and ASV.

	Background sample	Foreground sample
Age	39	30
Workclass	State-gov	Federal-gov
Education-Num	13	10
Marital Status	Never-married	Married-civ-spouse
Occupation	Adm-clerical	Adm-clerical
Relationship	Not-in-family	Own-child
Race	White	White
Sex	Male	Male
Capital Gain	2174	0
Capital Loss	0	0
Hours per week	40	40
Country	United-States	United-States

	Independent	On-manifold	ASV
Marital Status	0.03	0.08	0.03
Capital Gain	0.06	0.02	0.02
Workclass	0.03	0.03	0.02
Relationship	-0.01	-0.11	0.01
Education-Num	-0.02	0.01	-0.02
Age	-0.02	-0.03	0.01
Country	0.0	0.03	0.0
Capital Loss	0.0	0.03	0.0
Occupation	0.0	-0.03	0.0
Sex	0.0	0.03	0.0
Race	0.0	0.02	0.0
Hours per week	0.0	-0.0	0.0

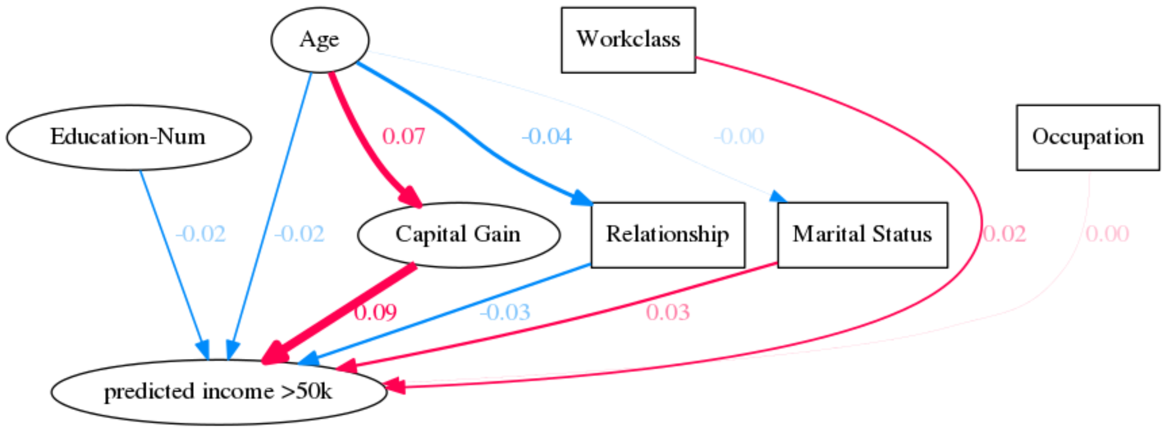

(a) Shapley Flow

Figure 13: Comparison between independent SHAP, on-manifold SHAP, ASV, and Shapley Flow on a sample from the income dataset. Shapley flow shows the top 10 links. Note that on-manifold gives non-zero attribution to even features that share the same value between background and foreground values (*e.g.*, country). Furthermore, although age appears to be not important directly, its impact through different causal edges are opposite as shown by Shapley Flow.

	Independent	On-manifold	ASV
Capital Gain	0.02	0.02	0.03
Education-Num	0.02	0.03	0.02
Age	0.01	0.01	0.01
Occupation	0.0	0.01	0.0
Capital Loss	0.01	-0.0	0.01
Relationship	0.01	0.0	0.0
Hours per week	0.0	0.01	-0.0
Sex	0.0	-0.01	0.0
Country	0.0	-0.01	0.0
Marital Status	-0.0	0.0	-0.0
Race	0.0	-0.01	-0.0
Workclass	0.0	-0.0	-0.0

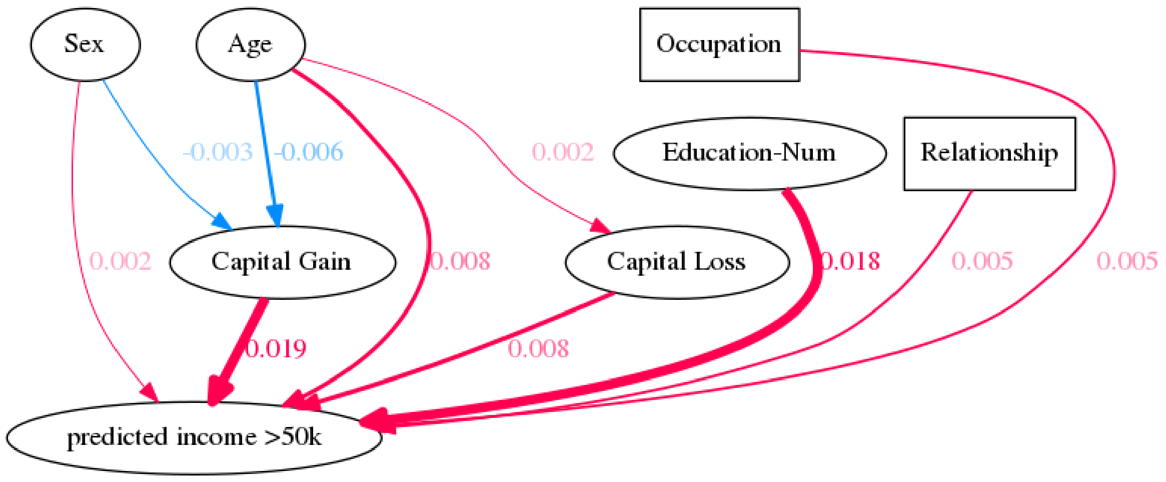

(a) Shapley Flow on the income data

Figure 14: Comparison of global understanding between independent SHAP, on-manifold SHAP, ASV, and Shapley Flow on the income dataset. Showing only the top 10 attributions for Shapley Flow for visual clarity.